Research article

Experimental and theoretical investigation of mild steel corrosion control in acidic solution by *Ranunculus arvensis* and *Glycine max* extracts as novel green inhibitors

Ghazal Sadat Sajadi [a], Razieh Naghizade [a], Leila Zeidabadinejad [a], Zahra Golshani [a], Mahnaz Amiri [b], Seyed Mohammad Ali Hosseini [a],[*]

[a] *Department of Chemistry, Shahid Bahonar University of Kerman, P.O. Box 76169-14111, Kerman, Iran*
[b] *Neuroscience Research Center, Institute of Neuropharmacology, Kerman University of Medical Science, Kerman, Iran*

A B S T R A C T

In the present research, the ability of *Ranunculus arvensis* (RA) and *Glycine max* (GM) extracts as green corrosion inhibitors of mild steel (MS) in 1 M HCl was investigated. The inhibiting potential of RA and GM was analysed employing electrochemical impedance spectroscopy (EIS), polarization curves, potentiometry, and theoretical investigations. An enhancement in the inhibition efficiency (I.E) with increasing inhibitors concentrations indicated by EIS data and polarization curves. According to obtained results both extracts indicated inhibitory effect, with their effectiveness following the order of RA > GM. In addition, the interactions between the inhibitors on the MS surface were assessed using B3LYP/6-311g(d,p) theory level in liquid water phase. The interaction energies for three orientations of RA and GM depicted that inhibitors have located parallel to the alloy surface. The preferred complex orientation is one in which the maximum number of inhibitor donor atoms interacted with the alloy surface. Finally, experimental and theoretical results were in accordance which confirmed the inhibition effect of RA and GM extracts.

1. Introduction

The inherent procedure of corrosion leads to the deterioration of exposed surfaces of refined metals to a form with more chemical stability in contact with gas or liquid due to the chemical reaction of oxidation between metals and their surroundings. Corrosion mainly results in significant economic losses, making it a dangerous phenomenon. The collapse of buildings and bridges, fracture of oil pipes, and flooding of sewerages are some consequences of corrosion [1]. The construction, nuclear, and petroleum industries use carbon steels as they are highly strong and cost-effective while also fabricated easily [2, 3, 4]. An aggressive media, including acidic solutions, used in different industrial processes to clean, pickle, and descale are challenging. Inhibitors can be used to efficiently decrease the corrosive effects on metals [4, 5, 6]. Organic compounds are typically considered as inhibitors of corrosive attacks in acidic solutions. The adsorption of organic compounds on the surface of metals is possible via heteroatoms, including N, S, P, and O, preventing the interaction of corrosive media with the active surface of metals [5, 6, 7, 8]. Yet, researchers seek to find more cost-effective,

environmentally friendly, and natural inhibiting factors because of the high costs and health-related problems brought by organic inhibitors [9, 10].

Inhibitors derived from natural products as well as renewable sources have been recently used by researchers to impose the minimum adverse environmental impacts [11, 12, 13, 14, 15]. According to Shahidi Zandi et al. [13], antibacterial medications can inhibit corrosion effectively concerning corrosion of steel in hydrochloric acid solutions, increasing their inhibitory effects when the concentration of the inhibitor increases. As depicted by them, these inhibitors had a maximum inhibitory efficiency of 98.4% when a concentration of 10 mM was considered. Ramezanzadeh et al. [14] considered *Urtica dioica* as an efficient corrosion inhibitor for mild steel (MS) in 1 M HCl solution, indicating the maximum inhibition efficiency of around 92% following a 2-hour immersion. As Golshani et al. [15] revealed, the extract of thyme affected corrosion of MS in acidic solutions substantially, achieving a 98% inhibition effectiveness in an inhibitor concentration of 200 ppm. According to Verma et al. [16], the leaves of *Glycine max* (GM) have the highest protection potential out of the extracts of *GM, Cuscuta reflexa,* and

---

Table 1. Chemical composition of the MS specimens.

Elements	Amount (wt. %)
Fe	97.84
Mn	1.4
Se	0.5
C	0.17
P	0.045
S	0.045

Table 2. Materials used in this study.

Materials	Ethyl alcohol	Hydrogen chloride acid	RA extract	GM extract
Purity percentage	96	37	–	–

Spirogyra extracts in an acidic environment. Given the acceptable inhibitory effects of GM leaves extract, the current research has used the extracts of GM seeds to investigate its inhibition effectiveness.

Researchers across the world are interested in soya bean due to the potential association of their consumption with decreased cancer risk as shown by epidemiologic investigations [17] while also reducing the risk of different diseases such as cardiovascular complications, menopause symptoms [18], and type II diabetes mellitus [19]. The extract obtained from the soya bean includes different flavonoids, including daidzein, glycitein, genistein, and so on as primary phytoconstituents [20].

Reports show that Ranunculus has had a long history of application in medical field due to biological functions, including anti-cancer, anti-inflammation, antioxidant, antibacterial, and anti-hypertension features [21]. Different members of Ranunculus show a variety of bioactivities primarily due to their bioactive phytochemical content [22]. Besides, *Ranunculus arvensis* (RA) possesses a moderate antiradical function [23].

We already investigated [24, 25, 26, 27, 28] the inhibitory effects of several organic inhibitors on metal corrosion behaviors; however, the current work aims to examine the impacts of RA and GM extracts on the alloy corrosion behavior in 1 M HCl to address the drawbacks of other broadly used corrosion inhibitors, including their high costs and environmentally adverse effects. The electrochemical impedance spectroscopy (EIS), potentiodynamic polarization, and potentiometry were employed to evaluate the performance of the inhibitor. The optical
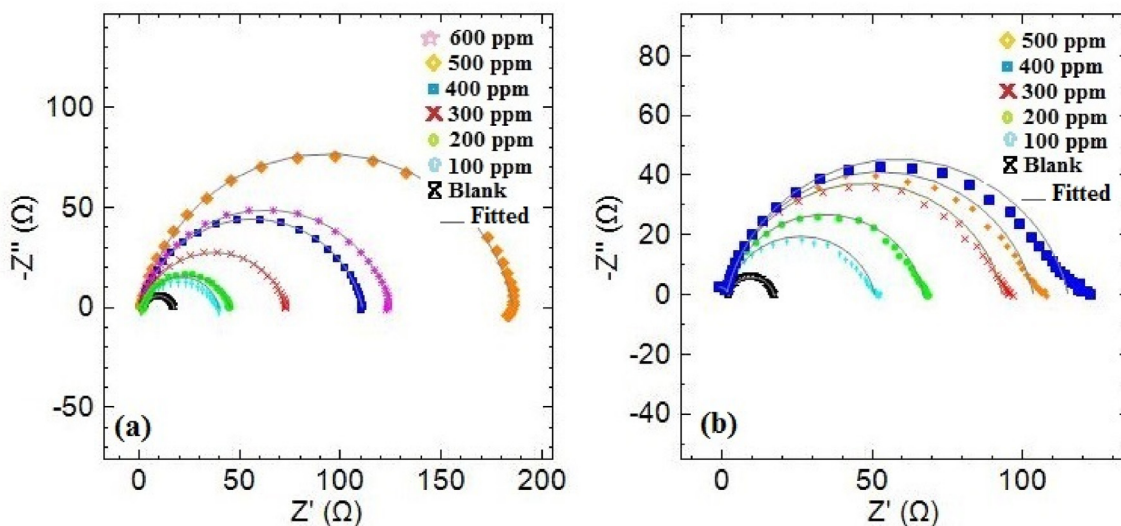
Figure 1. The Nyquist spectra of the MS alloy exposed in 1 M HCl with varies concentrations of (a) RA and (b) GM inhibitors.
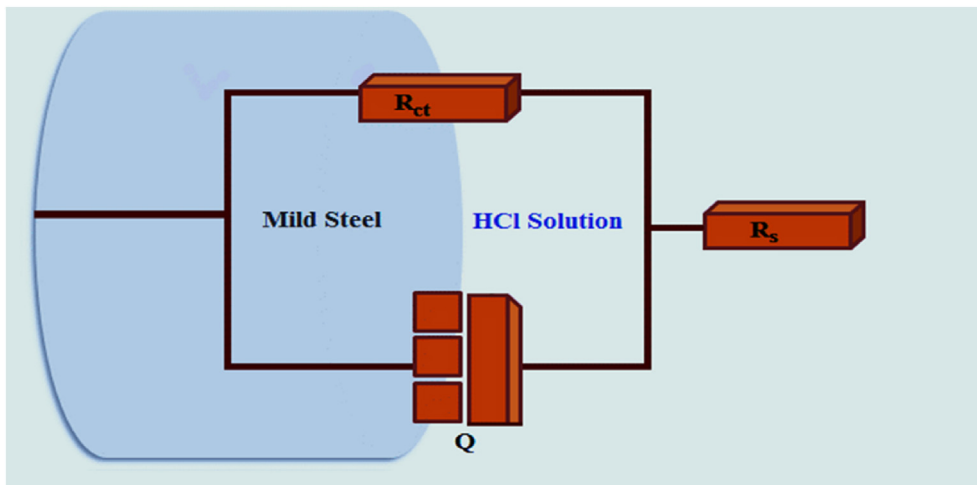
Figure 2. The electrical equivalent circuit used to obtain the EIS values.

Table 3. Corrosion quantities obtained from Nyquist plot of the MS in HCl in presence of different concentrations of RA and GM extracts.

Inhibitors	C/ppm	Rs/Ω. cm²	CPE		R_{ct}/Ω.cm²	C_{dl}/F.cm⁻²	X^2	IE%
			Y_0 (µF cm⁻²)	n				
Blank	–	1.79	399	0.857	15.1	69.32	0.105	–
RA	100	1.31	363	0.813	45.8	62.26	0.018	67.03
	200	1.33	353	0.822	48.9	51.54	0.046	69.12
	300	1.18	217	0.838	72.1	18.70	0.019	79.05
	400	1.28	91.3	0.878	109	5.80	0.009	86.14
	500	1.44	64.7	0.891	184	2.72	0.012	91.79
GM	100	1.37	126.277	0.861	56.88	16.43	0.037	73.45
	200	1.19	95.030	0.880	73.5	9.86	0.027	79.45
	300	1.19	78.802	0.872	98.8	6.87	0.035	84.71
	400	1.45	66.706	0.879	122.5	6.14	0.041	87.67
	500	1.25	83.920	0.868	109.44	7.87	0.036	86.20
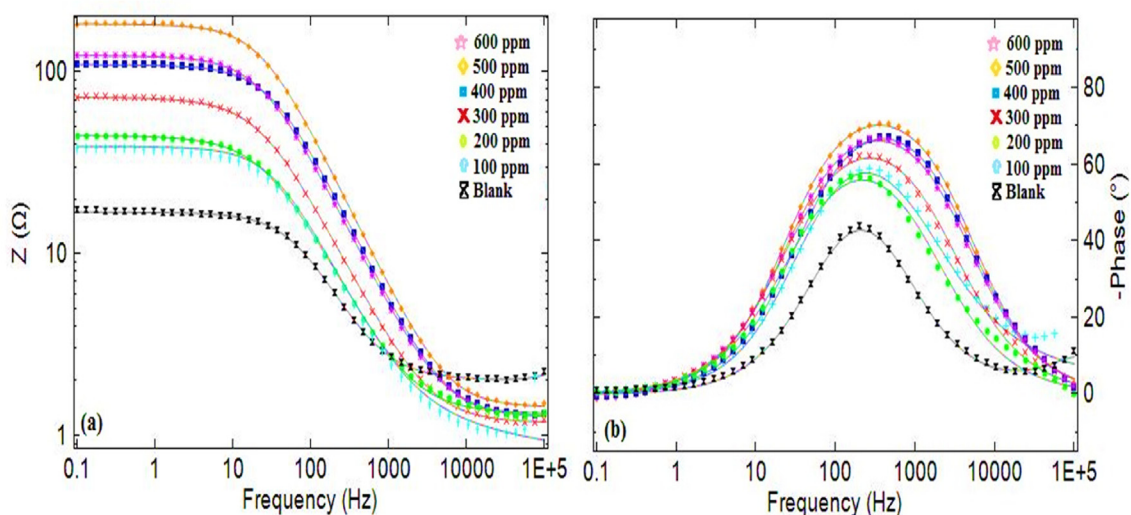
Figure 3. The impedance plots of the MS alloy exposed in 1 M HCl with different concentrations of RA extract; (a) Bode-magnitude, (b) Bode-phase plots.
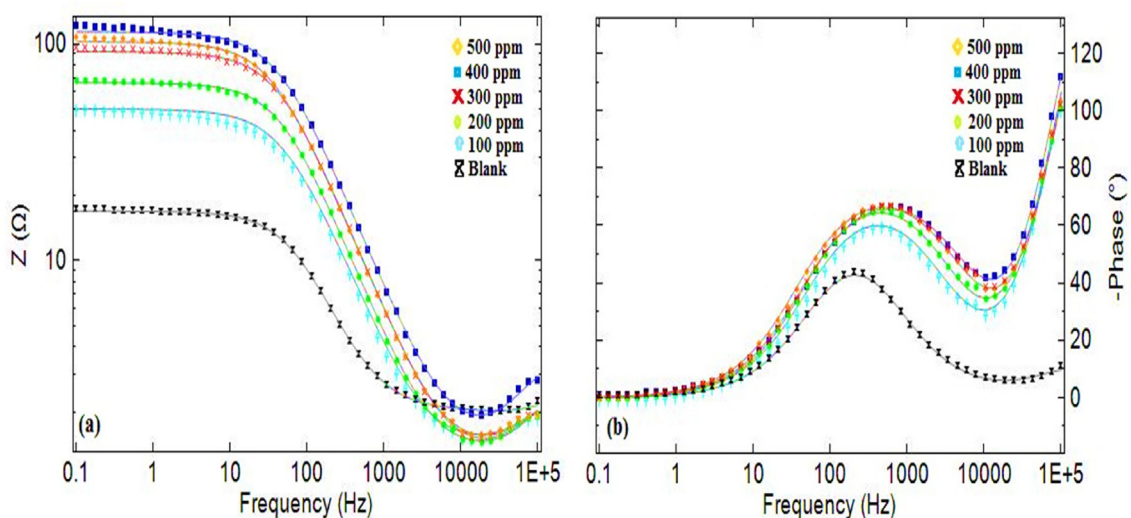
Figure 4. The impedance plots of the MS alloy exposed in 1 M HCl with different concentrations of GM extract; (a) Bode-magnitude, (b) Bode-phase plots.

microscopy (Leica zoom 2000 model) was also employed to investigate the function of RA and GM extracts in corrosion inhibition. Finally, the performance of the both extracts as corrosion inhibitors was investigated by quantum chemical methods, which has been expanded the relationship between inhibition efficiency of inhibitors with their molecular characters [29, 30, 31, 32, 33, 34].
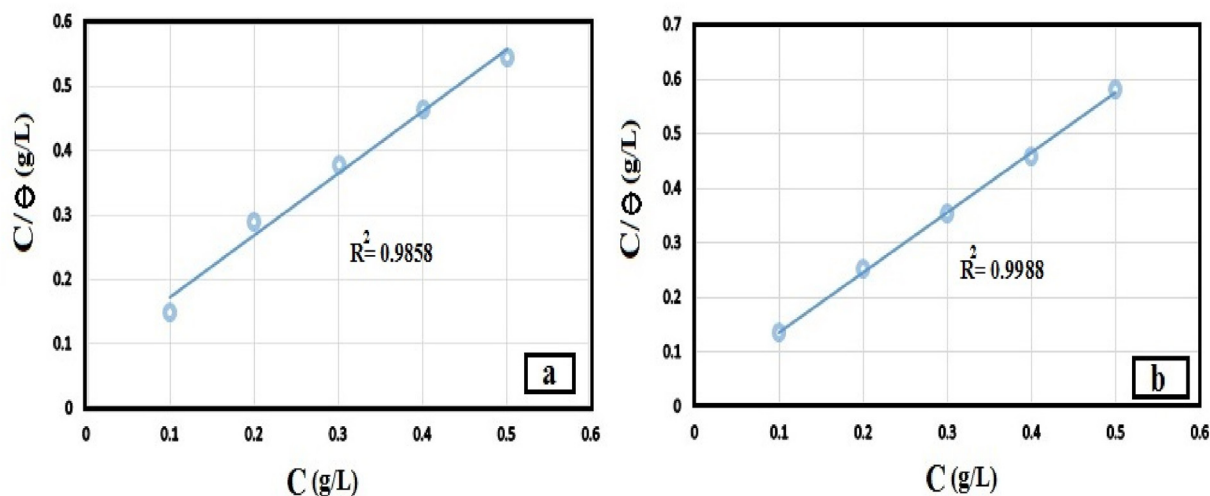
Figure 5. Langmuir adsorption isotherms of (a) RA and (b) GM inhibitor extracts from the EIS results on MS in 1 M HCl.

Table 4. Parameters obtained from Langmuir adsorption isotherms of RA and GM inhibitors on MS in 1 M HCl.

Inhibitors	Adsorption isotherm	Slope	K_{ads}	R^2	ΔG_{ads} (kJ/mol)
RA	Langmuir	0.966	13.23	0.9858	−16.35
GM	Langmuir	1.101	37.88	0.9988	−18.95

2. Material and methods

2.1. Preparation of the sample

All experiments were performed using MS samples with a 1-cm^2 area, along with chemical compositions represented in Table1. Mechanical abrasion of the samples was performed with 100–3000 grades of sand papers prior to experiments to achieve a considerable smooth surface, followed by ultrasonic degreasing with ethyl alcohol and then rinsing by deionized water.

2.2. Preparation of inhibitors

2.2.1. Ranunculus arvensis

RA extract prepared by the evaporation method. The healthy RA plant were collected from gardens around Kerman State-Iran. To eliminate dust, the plant was gently washed, dried in the shade at room temperature. In the next step, 100 g of dried RA plant were soaked in methanol for 72 h. After the filtration the surplus solvent was evaporated under reduced pressure in a rotary evaporator at 40 °C. The recovered residue had a consistent weight of 2.0 g [35].

2.2.2. Glycine max

GM seed purchased from the local markets in the Kerman, which are completely designated for commercial usage. To eliminate dust, GM were gently washed, dried in the shade at room temperature, then grounded and changed to powder form. At first, hexane and then methanol used for soaking. After evaporation of solvent by evaporator rotary device under low temperature and pressure, the remainder is used as a methanolic extract of GM [35].
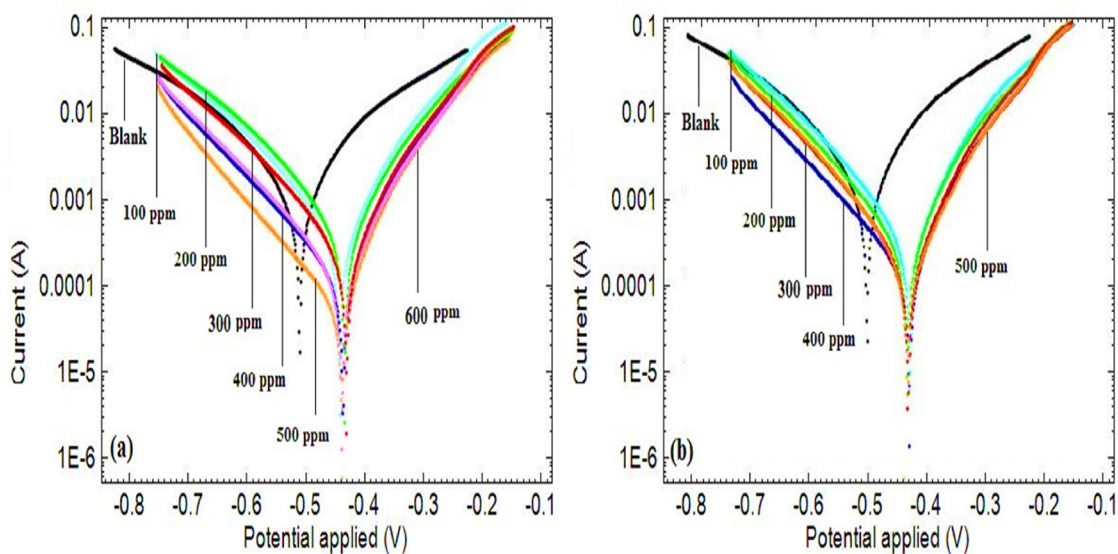
Figure 6. Potentiodynamic polarization curves of MS in 1 M HCl solution with and without of varies concentrations of a) RA and b) GM extract inhibitors.
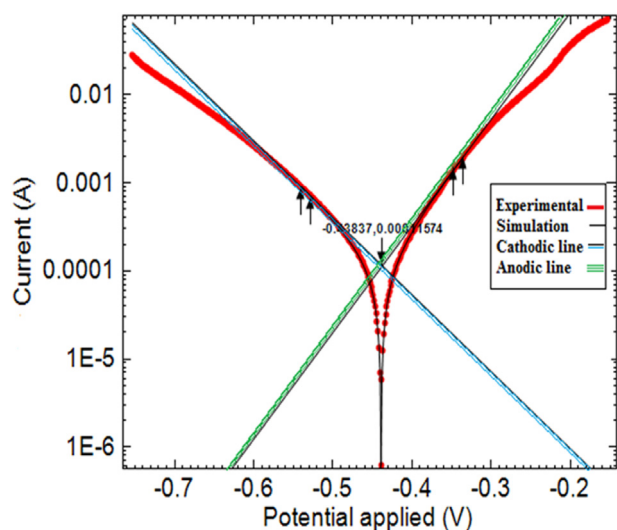
Figure 7. An instance of the non-linear fitting of potentiodynamic polarization curves.

Table 5. Electrochemical parameters obtained from polarization curves for mild steel in HCl in presence of different concentrations of RA and GM inhibitor extracts.

Inhibitors	C/ppm	i_{corr}/ $\mu A.cm^{-2}$	E_{corr}/ mv	β_a/ $mVdec^{-1}$	β_c/ $mVdec^{-1}$	IE%
Blank	–	1256	−511.3	136.3	90.70	–
RA	100	393.3	−435.6	150.7	92.38	68.68
	200	392.2	−434.8	164.0	94.44	68.77
	300	254.5	−431.4	164.2	96.62	79.73
	400	123.0	−437.7	165.6	96.21	90.20
	500	43.2	−438.5	165.7	97.51	96.56
GM	100	260.6	−439.2	117.6	77.0	79.25
	200	240.7	−441.0	127.1	81.86	80.83
	300	239.8	−436.2	127.6	82.1	80.90
	400	124.0	−437.4	130.1	137.1	90.13
	500	151.1	−440.0	103.6	80.54	87.96

2.3. Preparation of the electrolyte

Dilution of 37% HCl (supplied from Merck Co.) in deionized water was used to prepare the electrolyte for corrosion investigations, 1 M HCl.
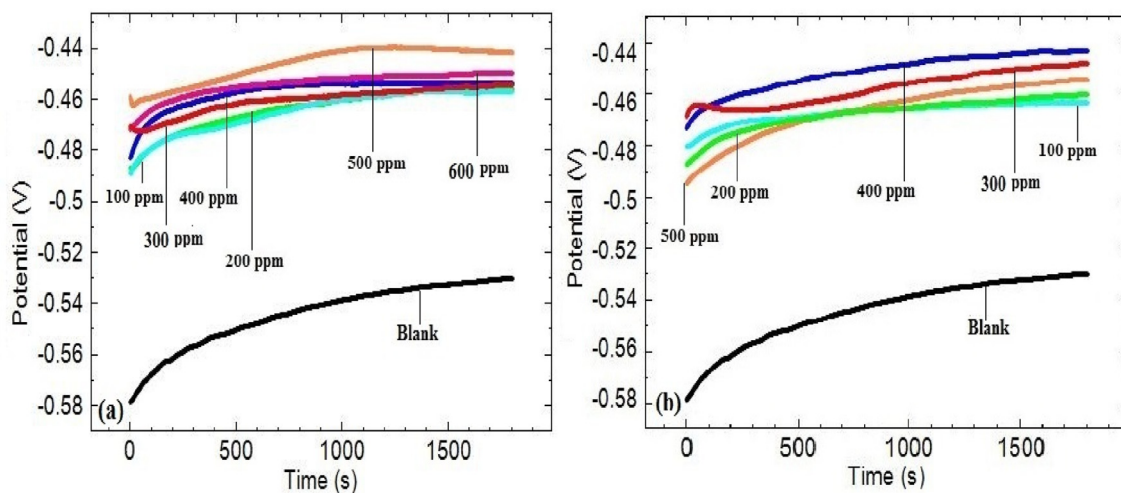
The both extracts as the inhibitor in the current study were added in the acidic solution, while electrolyte with no inhibitor was called blank solution. Concentrations of the inhibitor included 100, 200, 200, 400, 500 and 600 ppm/weight. All the materials used in this study along with purity percentage listed in Table 2:

2.4. Electrochemical analyses

An Autolab (302N Potentiostat model) device which had three-electrode system including Ag/AgCl electrode as a reference electrode (RE), platinum as a counter electrode, and MS as a working electrode (WE), was used to perform the electrochemical tests. A potential amplitude and frequency rate of 10 mV peak-to-peak and 10 mHz to 100 kHz were used, respectively, to measure the Alternate Current (AC) impedance. The polarization scan rate of 1 mV/s was considered for Tafel polarization curves, prepared through automatic changes in the electrode potential at a range of −250 to +250 mV versus E_{corr} at a temperature of 25 ± 1 °C. The measurement of the open circuit potential as a time function with and without the extract of inhibitors took place in 30-minute period. Besides, NOVA software was used to prepare the proper equivalent circuit and the respective EIS parameters. Three repetitions of experiments were performed to obtain reproducible results.

2.5. Characterization of the surface

Optical microscopy (Leica zoom 2000 model) and scanning electronic microscope (Sigma-Zeiss) were used to observe the morphologies and the EDX (energy dispersive X-ray spectroscopy) analysis of specimens prior to and following the addition of the both extracts to examine their performance as corrosion inhibitors. Accordingly, the immersion of working electrode was performed in 1 M HCl solution when the optimum concentrations of inhibitors were absent and present for around 24 h at ambient temperature. Removal and drying were the following steps.

2.6. Computational methods

Fully optimized geometries were done by the B3LYP/6-311G(d,p) level as performed in the Gaussian 09 suite of the program [36]. The basic structures of the Mild steel surface-RA and GM complexes, Only the 1:1 stoichiometric ratio are considered. The extracts were manually placed on the mild steel surface in three orientations. Physical and chemical properties such as, chemical potential (μ), hardness (η) and global electrophilicity index (ω) corresponding extracts, were studied.

Figure 8. OCP against time plots of MS in 1 M HCl without and with (a) RA and (b) GM inhibitor extracts.

After geometrical optimization step, the vibrational spectral analysis are done to ensure that the obtained optimum structures are at the level of potential energy.

2.7. Statistical analysis

After investigating the normal dissemination utilising Kolmogrov-Smearnov test, the data was subjected to One Way ANOVA and Tukey Post Hoc tests (sd = 0.05).

3. Results and discussion

3.1. Electrochemical corrosion behaviors

Different electrochemical procedures can be typically employed to evaluate the effectiveness of corrosion inhibitors.

3.1.1. Electrochemical impedance spectroscopy (EIS)

Information on the working electrode and HCl solution interface was provided using the EIS as a procedure with sufficient accuracy [37]. Figure 1(a) and (b) indicates the Nyquist plots derived from EIS of the MS in 1 M HCl solution when varies concentrations of RA and GM inhibitor extracts were used. According to this Figure, the Nyquist plots of the alloy in solutions with and without inhibitors indicated a single semi-circle characteristic. When inhibitors are added to the solution of HCl, the semi-circle diameter increases considerably, indicating the potential foundation of the protective layer on the surface of MS by the inhibitors and subsequent possibility of improving corrosion resistance in this solution [38].

Figure 1(a) and (b) indicates that the EIS data were matched by the electrical equivalent circuit presented in Figure 2. R_s, R_{ct}, and Q represent the electrolyte resistance, the charge transfer resistance, and the constant phase element developed because of double-layer (dl) presence, respectively in this equivalent circuit (Randles). The double layer capacitance (C_{dl}) values are computed by using Eq. (1) [39]:

$$C_{dl} = \left(Q_{CPE} \times R_{ct}^{1-n} \right)^{1/n} \qquad (1)$$

where Q, R_{ct} and n are the constant phase element, the charge transfer resistance, and the phase shift as regards the extent of surface inhomogeneity, respectively. The Q value can be calculated by admittance Y_0 and power n using the following formula [40]:

$$Q_{CPE} = Y_0(j\omega)^n \qquad (2)$$

In Eq. (2), j is the imaginary number ($j^2 = -1$), ω is the angular frequency in rad s^{-1}, n is the phase shift, for n = 0, CPE shows a resistance, for n = 1, a capacitance and for n = −1 an inductance. The dimension of Y_0 is sn/Ω, while that of a capacitance (C) is s/Ω or F. Despite this difference, Y_0 is often employed as if it were the capacitance of the corroding media [40]. Calculations of the protection efficiency (%IE) by R_{ct} in absence ($R_{ct,blk}$) and presence ($R_{ct,inh}$) of inhibitor extracts were performed using Eq. (3) [15]:

$$\%IE = \left(\frac{R_{ct,inh} - R_{ct,blk}}{R_{ct,inh}} \right) \times 100 \qquad (3)$$

Table 3 indicates the results of the EIS data fitting, the Randle circuit is best fitted over there providing good ($\chi2$) values, according to which adding the both extracts to the HCl solution led to an increase in the values of charge transfer resistance as well as inhibition effectiveness. At inhibitor concentrations 500 ppm for RA and 400 ppm for GM, R_{ct} reaches its maximum value, showing adsorption of more inhibitors and blockage of more active sites on the surface of the steel [41]. Also, by adding inhibitors, the value of R_s has not changed much. In addition, the value of C_{dl}, decreased by increasing concentration of extract, that can be related to decrease of local electric dl constant. The electrical double
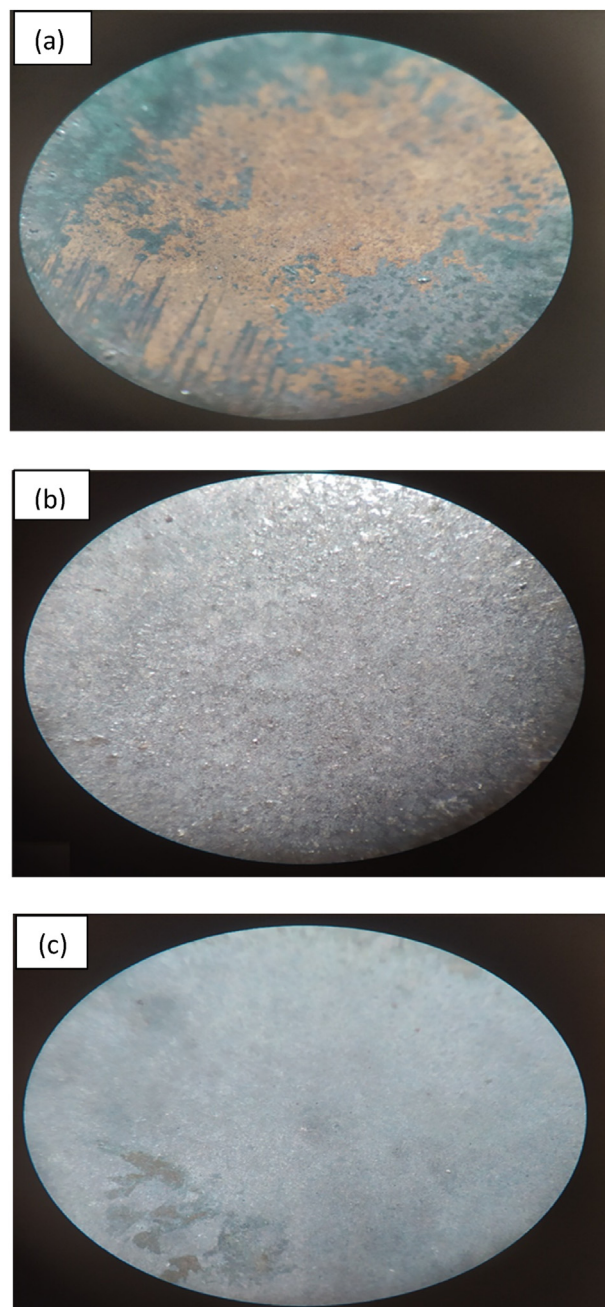
Figure 9. Optical microscopy images of MS surface in 1 M HCl solution in the (a) absence, (b and c) presence of RA and GM inhibitors, respectively.

layer value capacitance decreases with through increasing varies inhibitor concentrations, that is associated with the inhibitors molecules replacing the those of water adsorbed on the alloy surface, being indicative of a thicker layer between metal and solution [42].

Figures 3(a) and 4(a) illustrate MS Bode magnitude plots, that inhibitor concentrations of 500 ppm for RA and 400 ppm for GM show higher impedance values at low frequencies, indicating considerable resistance of the alloy in 1 M HCl solution [42]. Figures 3(b) and 4(b) illustrate Bode-phase plots for inhibited and uninhibited conditions, in which the single peak represents a single time-constant for the process of corrosion at the metal and solution interface [10]. Furthermore, when the extracts of RA and GM are added to the HCl solution, wider peak in the Bode-phase plots shifted to the higher frequency because the molecules of the inhibitor are adsorbed and a protective layer is formed on the alloy surface. Accordingly, the 500 ppm concentration of RA extract
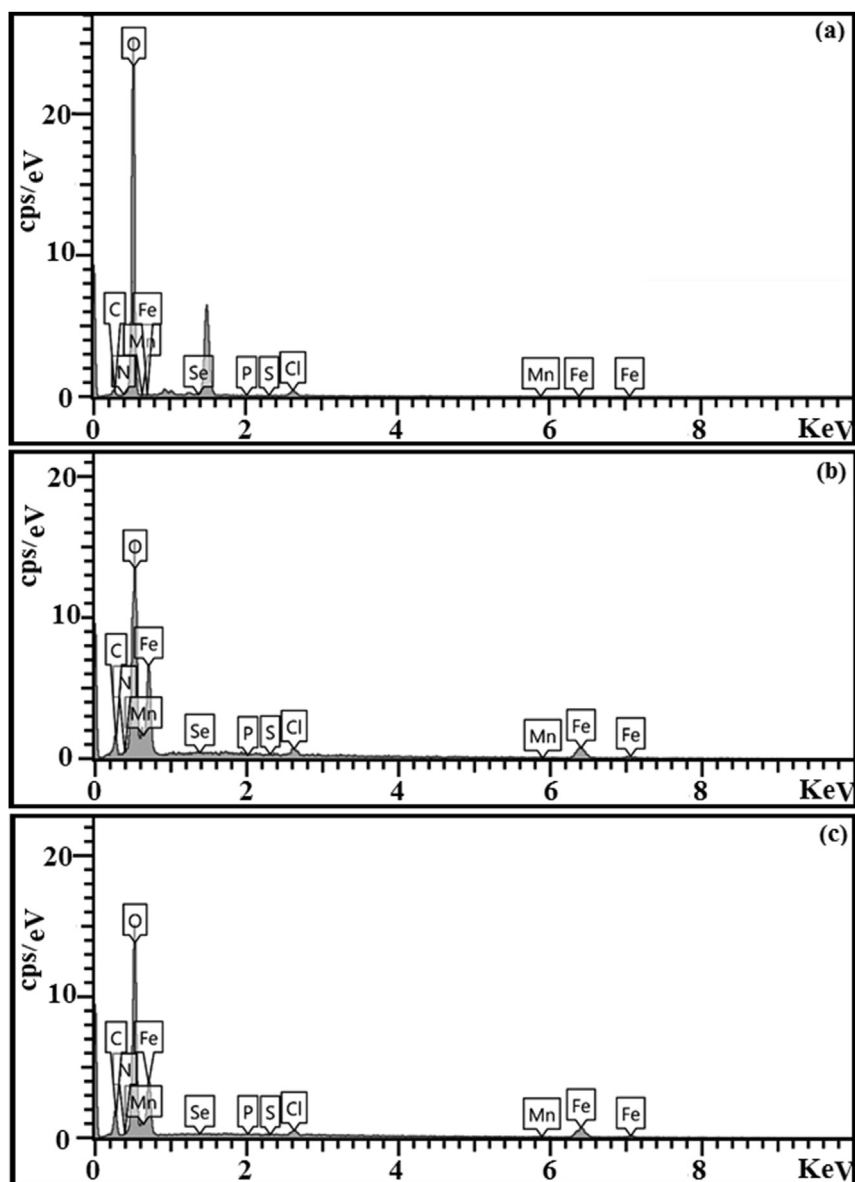
Figure 10. The spectrum of EDX for MS surface in 1 M HCl solution in the (a) absence, (b and c) presence of RA and GM inhibitors, respectively.

Table 6. EDX analysis values of MS surface in 1 M HCl without and with inhibitors, corresponding to Figure 10.

Inhibitors	Fe	O	C	Cl	Other
Blank	0.6	88.1	2.7	6.5	2.1
RA	54.4	40.0	3.6	1.8	0.2
GM	52.9	36.8	7.6	2.3	0.4

shows the highest inhibition effectiveness to diminish the corrosion rate of MS in hydrochloric acid solution [42, 43].

3.1.2. Adsorption isotherms

The inhibition of corrosion through RA and GM extracts is investigated according to adsorption of molecular. Previous researches [15, 44, 45] have illustrated adsorption isotherms to show the electron sharing between the molecules of inhibiting and the surfaces of alloy. To explain adsorption isotherms, the surface coating degree (θ) is calculated at various concentrations of RA and GM in the acidic media. The Temkin, Frumkin and Langmuir isotherm are the most frequently employed

models for recognizing adsorption; in this research, the Langmuir adsorption isotherm (derived from Eq. (4)) indicated the best achievement [44, 45].

$$\frac{C}{\theta} = \frac{1}{K_{ads}} + C \qquad (4)$$

In Eq. (4), θ shows the surface coating degree, C is the concentration of inhibitor, and K_{ads} is the constant of adsorption equilibrium. Therefore, considering C/θ plot in C, obtained by employing the EIS results (Figure 5a and b). A straight line in the graphs shows that the corrosion of MS alloy inhibited by RA and GM extracts.

The free energy of adsorption (ΔG_{ads}) is related to the K_{ads} and adsorption equilibrium of water. In addition, Eq. (5) is employed to obtained ΔG_{ads} [46, 47].

$$\Delta G_{ads} = -RTLn(55.5K_{ads}) \qquad (5)$$

55.5 is the water molar concentration in the 1 M HCl solution, R is the gas constant (8.314 J mol^{-1} K^{-1}), and T is the absolute temperature (K). The spontaneous inhibitors adsorption on the alloy surface can be revealed by the negative ΔG_{ads} value. Physical adsorption happens for
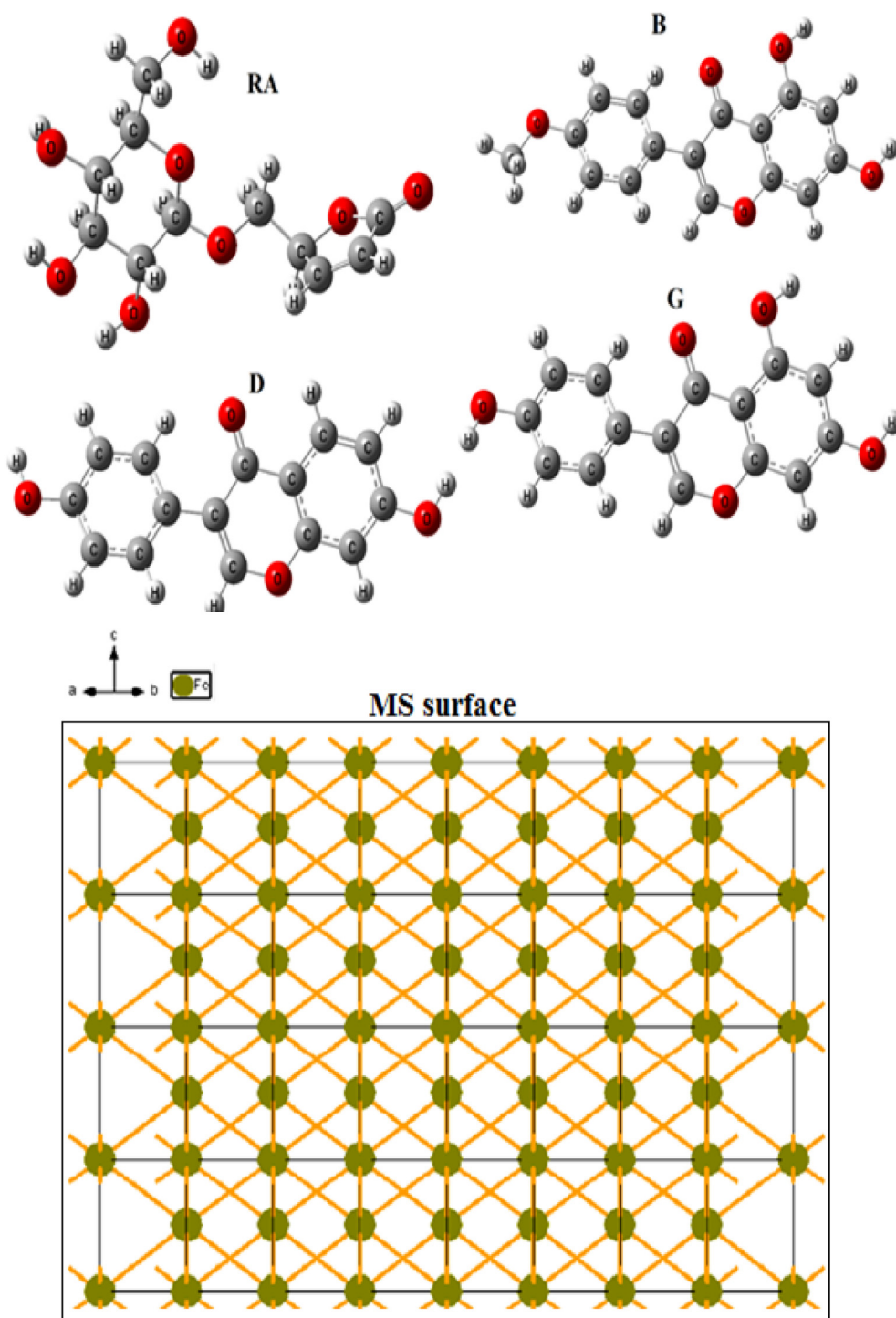
Figure 11. The structures of RA, B, D, G and the surface of MS that optimized by functional B3LYP.

ΔG_{ads} within the range 0 and -20 kJ/mol, while chemical adsorption happens when ΔG_{ads} is below -40 kJ/mol [48]. The ΔG_{ads} values in Table 4, -16.35 and -18.95 kJ/mol, representing that charge sharing between the both of extracts and the MS surface involve physical adsorption, which determines transfer from the inhibitor molecules on the alloy surface and the formation of a physical link.

3.1.3. Potentiodynamic polarization

Figure 6(a) and (b) represents the potentiodynamic polarization curves for MS in a solution of 1 M HCl for blank and different concentrations of RA and GM extracts. Accordingly, when the inhibitor extract is

present, the corrosion current density decreases, but there are no remarkable effects on the corrosion potential. Figure 7 shows an example of the non-linear fitting to obtain the kinetic parameters obtained from the potentiodynamic polarization.

Table 5 indicates the values of the corrosion potential (E_{corr}), corrosion current density (i_{corr}), cathodic and anodic Tafel slopes (βc and βa) and inhibition efficiency (%IE). Eq. (6) is used to calculate the %IE [15]:

$$\%IE = \left(\frac{i_{corr} - i_{inh}}{i_{corr}} \right) \times 100 \qquad (6)$$

In which, i_{corr} and i_{inh} represent the corrosion current densities taken
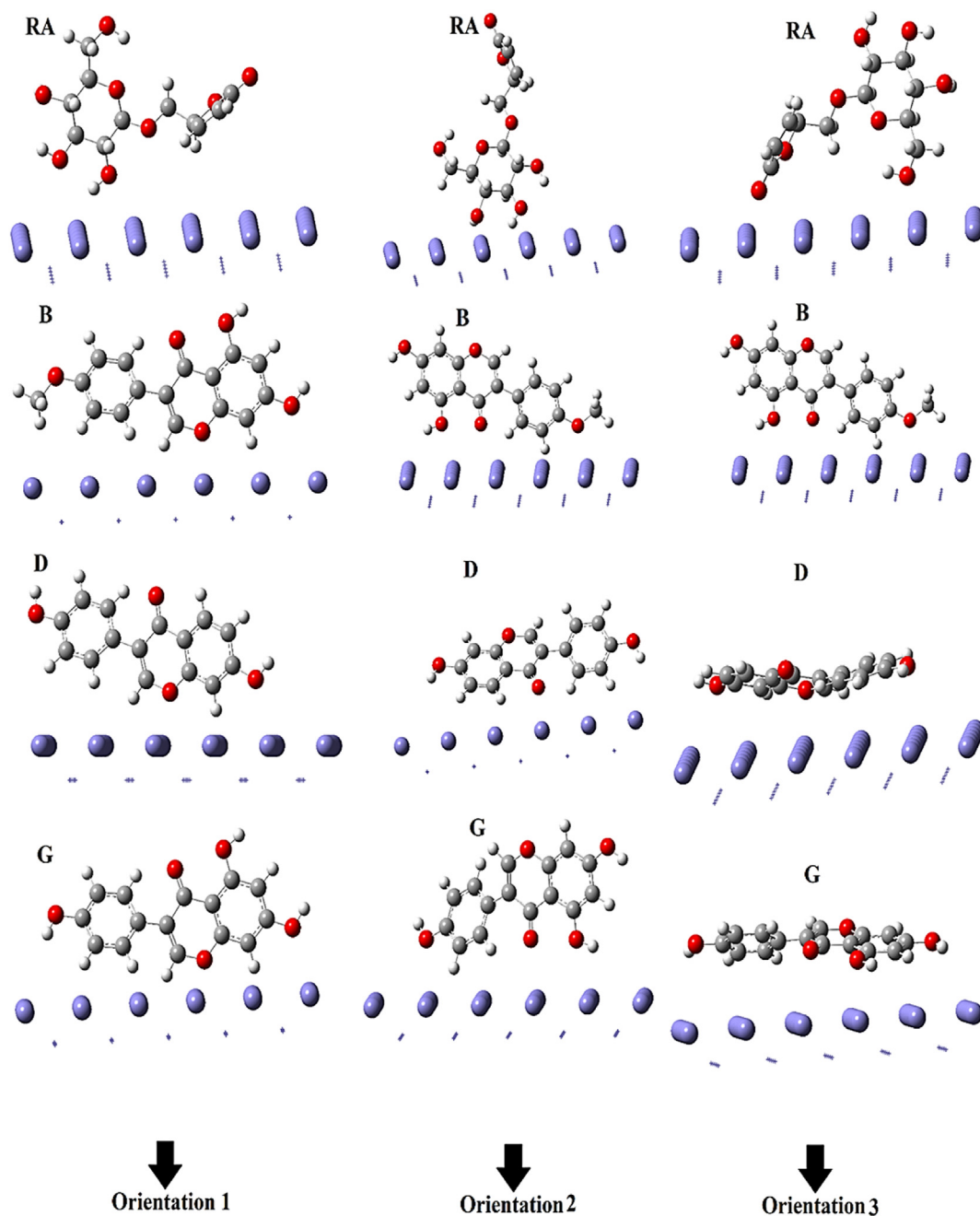
Figure 12. The important interaction between the surface of MS with RA, B, D and G in orientations (1), (2) and (3).

from blank and inhibited solutions, respectively. As shown in Figure 6 and Table 5, the inhibitor has higher effectiveness when concentration of inhibitor reaches a peak of 500 ppm RA and 400 ppm GM extracts, correspondingly, with respective inhibitor effectiveness of 96.56% and 90.13%.

The results of Table 5 indicate that as the concentration of inhibitors in blank solution increases, there is a gradual increase in ßa and ßc. Therefore, both of the extracts had some effects on both anodic and cathodic reactions. There is a minimum effect of RA and GM inhibitor extracts on corrosion potential. Nevertheless, adding the inhibitors to the HCl solution led to a considerable decrease in the MS corrosion rate. According to the polarization findings, in 500 ppm of RA and 400 ppm of GM extract concentrations, the least corrosion rate can be observed. Therefore, the development of adsorption film of the extracts indicates activation of the blocking effects while reducing alloy corrosion rates

[49]. These results are in accordance with the findings obtained from EIS analysis, indicating the effectiveness of the two extracts as corrosion inhibitors.

3.1.4. Potentiometry

Various values of OCP over time are given in Figure 8 for MS in blank solution, as well as respective RA and GM inhibitors concentrations. Obviously, the primary surge in the OCP of blank and solutions including inhibitor concentrations is because of the oxide film formation and the inhibitor molecules adsorption on the metal surface, respectively. When RA and GM inhibitors are present in the solutions, the potential in steady state shifts towards more positive values with no changes in the overall characteristics of the Potentiometry curve. Hence, inhibitor's protecting film is formed and thickened on the alloy surface, the cathodic exchange current density decreases which consequently increases the E_{corr} [50, 51].

Table 7. The interaction energy of G, D, B and RA with the MS surface in eV.

complexes	G-MS surface	D-MS surface	B-MS surface	RA-MS surface
Orientation 1	−0.15	−0.16	−0.14	−0.16
Orientation 2	−0.17	−0.11	−0.18	−0.17
Orientation 3	−0.54	−0.46	0.41	−0.22

3.2. Surface morphology of MS

RA and GM extract adsorbed on MS surface leads to inhibition of the alloy in the solution and this was investigated by optical microscopy analysis. The inhibitor films comprised of RA or GM molecules are accomplished on the surface of the alloy, which are spontaneous physical adsorption. The optical image of MS sample exposed in 1 M HCl media illustrated harmed and atypical surface because of the chloride ions aggressive attack in acidic media (Figure 9a). In addition, the metal surface in present of RA and GM inhibitors showed in Figure 9b and c, respectively with comparatively smooth surface, which validated the present of an effective film of RA and GM on MS surface that protected the MS surface from the aggressive acidic solution [15].

3.3. EDX analysis of MS

According to EDX spectra, it is available to find the corrosion composition of elements on the surface of MS by aggressive media. The EDX spectra of the alloy surface after 24 h immersion in 1.0 M HCl solution without, and with optimum concentrations of inhibitors are shown in Figure 10, the composition of elements is given in Table 6. Figure 10(a) shows corrosion product of MS, and illustrated a signal value of iron (0.6%). Although in solution with inhibitors the value of Fe atom enhanced strongly, and the carbon peak increased clearly due to the molecules adsorption of inhibitor on the alloy surface. The signals of oxygen detected in HCl, and solution with inhibitors, were taken from the complex oxides, and/or hydroxides formed on the alloy surface. In presence of inhibitors in acid solution, the chlorine peak was obviously decreased and chlorine value was distinctly depressed (Figure 10b and c). From the obtained results, it is validating that the molecules of inhibitor were adsorbed on the alloy surface, hence the MS corrosion successfully inhibited in 1 M HCl by the both of extracts [52].

3.4. Theoretical analysis

3.4.1. Molecular geometry and energy analysis

The purpose of this work is to describe the electronic and structural nature of the interactions between mild steel surfaces with different orientations of RA and GM extracts. The functional B3LYP was chosen to review its adequacy to the relevant structures. Supercell MS was selected in the size of $(4 \times 4 \times 2)$. All the considered structures are shown in Figure 11. Major constituents of soya beans contain large amounts of nutrients, such as proteins and flavonoids, including genistein (G), daidzein (D) and biochanin A (B). Oxygen atoms from the G, D, B and RA can react to the surface of alloy (Figure 11).

The oxygen atoms of the hydroxyl and ketone groups of inhibitors interact in various directions with the steel surface. Three perpendicular

(1, 2), and parallel (3) orientations are proposed for inhibiting molecules as shown in Figure 12. In Table 7, the inhibitor molecules interactions were given. From Table 7 and Figure 12 it is observed that all inhibitory molecules are adsorbed on MS surface with approximately parallel or flat locations. Strong interactions between iron surface atoms and inhibitors occur when the inhibitors are adsorbed parallel with the alloy surface. The most important interactions are among the oxygen atoms of the hydroxyl and ketone groups of GM molecules in orientation 3, and so oxygen atoms of the hydroxyl groups of RA in orientation 3.

3.4.2. HOMO-LUMO parameters

For analysing the electronic transitions nature in GM and RA/MS surface complexes, molecular attributes such as orbital energies can be used, HOMO the ionization potential (I) can be defined as: $I = -E_{HOMO}$ and electron affinity (A) and $A = -E_{LUMO}$. The attributes of molecular, for intance chemical potential, are computed by using Eq. (7) [31]:

$$\mu = \frac{(I + A)}{2} \tag{7}$$

The hardness (η) as Eq. (8):

$$\eta = \frac{(I - A)}{2} \tag{8}$$

And indicator of global electrophilicity (ω) as Eq. (9):

$$\omega = \frac{\mu^2}{2\eta} \tag{9}$$

The energy levels of frontier molecular orbitals are an valuable information, which can be employed as an index of consistency and chemical reactivity of the inhibitors. Therefore, one can discover how GM and RA molecules with MS surface interact and where the are active sites in inhibitors. The gap energy of the frontier molecular orbitals E_{HOMO} and E_{LUMO} (E_g), Dipole moment (D), electronic potential (μ), hardness (η) and global electrophilicity index (ω) for the inhibitors and complexes are computed and listed in Table 8.

Table 8 shows the values of molecular descriptors indicating the electron charge transfer from HOMO to the orbital LUMO, that has an impact on the activity and structure of the inhibitory electron molecule. The μ values indicate that the alloy surface is electron accepting. These outcomes are in accordance with the values in Table 8, and μ less than zero indicates a spontaneous reaction. The larger global electrophilic index ($\omega > 2$ eV) illustrates that the interaction among the inhibitors and the alloy surface is of interest.

4. Conclusion

In this research, RA and GM extracts as cost-effective green inhibitors were prepared by the easy extraction-evaporation technique. The inhibition ability of the inhibitors assessed via both experimental and theoretical (DFT simulations) methods, corrosion inhibiting mechanism of the extracts for MS were investigated as well. EIS and Tafel results indicated that RA and GM are acceptable inhibitors, which could sustainably inhibit the anodic and cathodic reaction of the alloy.

- EIS findings indicated a considerable inhibition efficiency equal to 91.79% and 87.67% in 500 ppm of RA and 400 ppm of GM extract concentrations, respectively because of the extract molecules adsorption on the alloy surface.
- The adsorption of the both inhibitors on the alloy surface followed the Langmuir isotherm. And, the extracts on the metal surface showed physical adsorption.
- Based on polarization methods, the extracts were mixed type inhibitors for MS in an acidic environment that could significantly decrease the current density of the MS surface and further decrease the dissolution rate of the alloy in the HCl.

Table 8. Frontier molecular orbital Energies HOMO–LUMO gap and global reactivity descriptors for interactions between RA, B, D, and G with the MS surface.

	E_g (eV)	Dipole moment	η (eV)	μ (eV)	ω (eV)
Mild steel surface	0.1124	0.4252	0.0561	−5.8731	307.4269
RA	6.0632	5.9972	3.0316	−4.4240	3.2279
G	4.2841	3.7685	2.1420	−3.3867	2.6772
D	4.1110	2.1741	2.0555	−3.5810	3.1192
B	4.2403	3.2411	2.1201	−3.3346	2.6223

- The results of surface morphology analysis were in accordance with electrochemical data and confirmed the inhibition ability of extracts.
- According to the theoretical investigation, values of electronic potential validate that the electrons were accepted by the surface of MS. This result is consistent with the complexation energy, and electronic potential.
- There is the specific correlation between the experimental and empirical results through theoretical calculations of quantum chemical parameters.

Declarations

Author contribution statement

Ghazal Sadat Sajadi, Seyed Mohammad Ali Hosseini: Conceived and designed the experiments; Performed the experiments; Analyzed and interpreted the data; Contributed reagents, materials, analysis tools or data; Wrote the paper.

Razieh Naghizade, Leila Zeidabadinejad, Zahra Golshani, Mahnaz Amiri: Conceived and designed the experiments; Wrote the paper.

Data availability statement

Data included in article/supplementary material/referenced in article.

Declaration of interests statement

The authors declare no conflict of interest.

Additional information

No additional information is available for this paper.

References

[1] W.S. Tait, Electrochemical corrosion basics, in: Handbook of Environmental Degradation of Materials, Elsevier, 2018, pp. 97–115.

[2] A. Fouda, A. Ellithy, Inhibition effect of 4-phenylthiazole derivatives on corrosion of 304L stainless steel in HCl solution, Corrosion Sci. 51 (4) (2009) 868–875.

[3] K. Azzaoui, E. Mejdoubi, S. Jodeh, A. Lamhamdi, E. Rodriguez-Castellón, M. Algarra, A. Zarrouk, A. Errich, R. Salghi, H. Lgaz, Eco friendly green inhibitor Gum Arabic (GA) for the corrosion control of mild steel in hydrochloric acid medium, Corrosion Sci. 129 (2017) 70–81.

[4] P. Singh, M. Quraishi, Corrosion inhibition of mild steel using Novel Bis Schiff's Bases as corrosion inhibitors: electrochemical and surface measurement, measurement 86 (2016) 114–124.

[5] Z. Salarvand, M. Amirnasr, M. Talebian, K. Raeissi, S. Meghdadi, Enhanced corrosion resistance of mild steel in 1 M HCl solution by trace amount of 2-phenyl-benzothiazole derivatives: experimental, quantum chemical calculations and molecular dynamics (MD) simulation studies, Corrosion Sci. 114 (2017) 133–145.

[6] N. Caliskan, E. Akbas, The inhibition effect of some pyrimidine derivatives on austenitic stainless steel in acidic media, Mater. Chem. Phys. 126 (3) (2011) 983–988.

[7] E. Gutiérrez, J.A. Rodríguez, J. Cruz-Borbolla, J.G. Alvarado-Rodríguez, P. Thangarasu, Development of a predictive model for corrosion inhibition of carbon steel by imidazole and benzimidazole derivatives, Corrosion Sci. 108 (2016) 23–35.

[8] A. Döner, R. Solmaz, M. Özcan, G. Kardas, Experimental and theoretical studies of thiazoles as corrosion inhibitors for mild steel in sulphuric acid solution, Corrosion Sci. 53 (9) (2011) 2902–2913.

[9] N. Soltani, N. Tavakkoli, M. Khayatkashani, M.R. Jalali, A. Mosavizade, Green approach to corrosion inhibition of 304 stainless steel in hydrochloric acid solution by the extract of Salvia officinalis leaves, Corrosion Sci. 62 (2012) 122–135.

[10] P. Mourya, S. Banerjee, M. Singh, Corrosion inhibition of mild steel in acidic solution by Tagetes erecta (Marigold flower) extract as a green inhibitor, Corrosion Sci. 85 (2014) 352–363.

[11] A. Thakur, A. Kumar, Sustainable inhibitors for corrosion mitigation in aggressive corrosive media: a comprehensive study, J. Bio- Tribo-Corrosion 7 (2021) 1–48.

[12] S. Bashir, A. Thakur, H. Lgaz, I.-M. Chung, A. Kumar, Corrosion inhibition performance of acarbose on mild steel corrosion in acidic medium: an experimental and computational study, Arab. J. Sci. Eng. 45 (2020) 4773–4783.

[13] G. Golestani, M. Shahidi, D. Ghazanfari, Electrochemical evaluation of antibacterial drugs as environment-friendly inhibitors for corrosion of carbon steel in HCl solution, Appl. Surf. Sci. 308 (2014) 347–362.

[14] M. Ramezanzadeh, G. Bahlakeh, Z. Sanaei, B. Ramezanzadeh, Studying the Urtica dioica leaves extract inhibition effect on the mild steel corrosion in 1 M HCl solution: complementary experimental, ab initio quantum mechanics, Monte Carlo and molecular dynamics studies, J. Mol. Liq. 272 (2018) 120–136.

[15] Z. Golshani, H.C. Moezabad, M. Amiri, G.S. Sajadi, R. Naghizade, S.M. Hosseini, Effect of Thyme extract as an ecofriendly inhibitor for corrosion of mild steel in acidic media, Mater. Corros. 73 (2022) 460–469.

[16] D. Verma, F. Khan, I. Bahadur, M. Salman, M. Quraishi, C. Verma, E.E. Ebenso, Inhibition performance of Glycine max, Cuscuta reflexa and Spirogyra extracts for mild steel dissolution in acidic medium: density functional theory and experimental studies, Results Phys. 10 (2018) 665–674.

[17] D. Ingram, K. Sanders, M. Kolybaba, D. Lopez, Case-control study of phyto-oestrogens and breast cancer, Lancet 350 (1997) 990–994.

[18] H. Adlercreutz, E. Hämäläinen, S. Gorbach, B. Goldin, Dietary phyto-oestrogens and the menopause in Japan, Lancet 339 (1992) 1233.

[19] F.A. Van De Laar, P.L. Lucassen, R.P. Akkermans, E.H. Van De Lisdonk, G.E. Rutten, C. Van Weel, α-Glucosidase inhibitors for patients with type 2 diabetes: results from a Cochrane systematic review and meta-analysis, Diabetes Care 28 (2005) 154–163.

[20] H.J. Yuk, J.H. Lee, M.J. Curtis-Long, J.W. Lee, Y.S. Kim, H.W. Ryu, C.G. Park, T.-S. Jeong, K.H. Park, The most abundant polyphenol of soy leaves, coumestrol, displays potent α-glucosidase inhibitory activity, Food Chem. 126 (2011) 1057–1063.

[21] D.-c. Hao, P.-g. Xiao, Pharmaceutical resource discovery from traditional medicinal plants: pharmacophylogeny and pharmacophylogenomics, Chin. Herbal Med. 12 (2020) 104–117.

[22] M.S. Aslam, B.A. Choudhary, M. Uzair, A.S. Ijaz, The genus Ranunculus: a phytochemical and ethnopharmacological review, Int. J. Pharm. Pharmaceut. Sci. 4 (2012) 15–22.

[23] M.Z. Khan, S. Jan, F.U. Khan, W. Noor, Y.M. Khan, A. Shah, M. Chaudhary, F. Ali, K. Khan, W. Ullah, Phytochemical screening and biological activities of Ranunculus arvensis, Int. J. Biol. Sci. 11 (2017) 15–21.

[24] S. Hosseini, M. Mousavi, M. Amiri, The corrosion inhibition of Ti-alloy (VT-9) in mixture of H2SO4-NaF by organic compounds, Protect. Met. Phys. Chem. Surf. 45 (2009) 461–465.

[25] S. Hosseini, M. Amiri, Electrochemical and dissolution behavior of the Ti-alloy VT-9 in H2SO4 solution in the presence of the organic inhibitor (2-phenyl-4-[(E)-1-(4-solphanylanilino) methylyden]-1, 3-oxazole-5 (4H)-one, J. Iran. Chem. Soc. 4 (2007) 451–458.

[26] S. Hosseini, M. Amiri, A. Momeni, Inhibitive effect of L–OH on the corrosion of austenitic chromium–nickel steel in H 2 SO 4 solution, Surf. Rev. Lett. 15 (2008) 435–442.

[27] S. Eftekhar, M. Amiri, Polarization behaviour of stainless steel type 302 in HCl solution of benzotriazole, Asian J. Chem. 19 (2007) 2574.

[28] M. Bahrami, S. Hosseini, P. Pilvar, Experimental and theoretical investigation of organic compounds as inhibitors for mild steel corrosion in sulfuric acid medium, Corrosion Sci. 52 (2010) 2793–2803.

[29] M. Abreu-Quijano, M. Palomar-Pardavé, A. Cuán, M. Romero-Romo, G. Negrón-Silva, R. Álvarez-Bustamante, A. Ramírez-López, H. Herrera-Hernández, Quantum chemical study of 2-mercaptoimidazole, 2-Mercaptobenzimidazole, 2-Mercapto-5-Methylbenzimidazole and 2-Mercapto-5-Nitrobenzimidazole as corrosion inhibitors for steel, Int. J. Electrochem. Sci. 6 (2011) 3729–3742.

[30] O. Senhaji, R. Taouil, M. Skalli, M. Bouachrine, B. Hammouti, M. Hamidi, S. Al-Deyab, Experimental and theoretical study for corrosion inhibition in normal hydrochloric acid solution by some new phophonated compounds, Int. J. Electrochem. Sci. 6 (2011) 6290.

[31] L. Zeidabadinejad, S.M.A. Hosseini, Computational study of inhibitory effect of urea, n-allylthiourea, thiosemicarbazide, and phenylhydrazine on the aluminum surfaces, Mater. Corros. 70 (2019) 1715–1725.

[32] A. Thakur, S. Kaya, A. Abousalem, S. Sharma, R. Ganjoo, H. Assad, A. Kumar, Computational and experimental studies on the corrosion inhibition performance of an aerial extract of Cnicus Benedictus weed on the acidic corrosion of mild steel, Process Saf. Environ. Protect. 161 (2022) 801–818.

[33] S. Bashir, A. Thakur, H. Lgaz, I.-M. Chung, A. Kumar, Computational and experimental studies on Phenylephrine as anti-corrosion substance of mild steel in acidic medium, J. Mol. Liq. 293 (2019), 111539.

[34] S. Bashir, A. Thakur, H. Lgaz, I.-M. Chung, A. Kumar, Corrosion inhibition efficiency of bronopol on aluminium in 0.5 M HCl solution: insights from experimental and quantum chemical studies, Surface. Interfac. 20 (2020), 100542.

[35] R.R. Chattopadhyay, Possible mechanism of hepatoprotective activity of Azadirachta indica leaf extract: part II, J. Ethnopharmacol. 89 (2003) 217–219.

[36] S. McArdle, S. Endo, A. Aspuru-Guzik, S.C. Benjamin, X. Yuan, Quantum computational chemistry, Rev. Mod. Phys. 92 (2020), 015003.

[37] M.M.K. Azar, H.S. Gugtapeh, M. Rezaei, Evaluation of corrosion protection performance of electroplated zinc and zinc-graphene oxide nanocomposite coatings in air saturated 3.5 wt.% NaCl solution, Colloids Surf. A: Physicochem. Eng. Aspects 601 (2020), 125051.

[38] A. Dehghani, G. Bahlakeh, B. Ramezanzadeh, M. Ramezanzadeh, Potential of Borage flower aqueous extract as an environmentally sustainable corrosion

inhibitor for acid corrosion of mild steel: electrochemical and theoretical studies, J. Mol. Liq. 277 (2019) 895–911.

[39] S. Martinez, M. Metikoš-Huković, A nonlinear kinetic model introduced for the corrosion inhibitive properties of some organic inhibitors, J. Appl. Electrochem. 33 (2003) 1137–1142.

[40] C. Shan, X. Hou, K.-L. Choy, Corrosion resistance of TiO2 films grown on stainless steel by atomic layer deposition, Surf. Coating. Technol. 202 (2008) 2399–2402.

[41] C.M. Fernandes, L.V. Faro, V.G. Pina, M.C.B. de Souza, F.C. Boechat, M.C. de Souza, M. Briganti, F. Totti, E.A. Ponzio, Study of three new halogenated oxoquinolinecarbohydrazide N-phosphonate derivatives as corrosion inhibitor for mild steel in acid environment, Surf. Interfaces 21 (2020), 100773.

[42] H. Hamani, T. Douadi, M. Al-Noaimi, S. Issaadi, D. Daoud, S. Chafaa, Electrochemical and quantum chemical studies of some azomethine compounds as corrosion inhibitors for mild steel in 1 M hydrochloric acid, Corrosion Sci. 88 (2014) 234–245.

[43] Y. Qiang, S. Zhang, B. Tan, S. Chen, Evaluation of Ginkgo leaf extract as an ecofriendly corrosion inhibitor of X70 steel in HCl solution, Corrosion Sci. 133 (2018) 6–16.

[44] R.K. Ahmed, S. Zhang, Alchemilla vulgaris extract as green inhibitor of copper corrosion in hydrochloric acid, Int. J. Electrochem. Sci. 14 (2019) 10657–10669.

[45] Y. Qiang, S. Zhang, H. Zhao, B. Tan, L. Wang, Enhanced anticorrosion performance of copper by novel N-doped carbon dots, Corrosion Sci. 161 (2019), 108193.

[46] B. Tan, S. Zhang, W. Li, X. Zuo, Y. Qiang, L. Xu, J. Hao, S. Chen, Experimental and theoretical studies on inhibition performance of Cu corrosion in 0.5 M H2SO4 by three disulfide derivatives, J. Ind. Eng. Chem. 77 (2019) 449–460.

[47] M. Javidi, R. Omidvar, Synergistic inhibition behavior of sodium tungstate and penicillin G as an eco-friendly inhibitor on pitting corrosion of 304 stainless steel in NaCl solution using Design of Experiment, J. Mol. Liq. 291 (2019), 111330.

[48] Y. Qiang, S. Zhang, L. Wang, Understanding the adsorption and anticorrosive mechanism of DNA inhibitor for copper in sulfuric acid, Appl. Surf. Sci. 492 (2019) 228–238.

[49] E.E. Oguzie, J. Li, Y. Liu, D. Chen, Y. Li, K. Yang, F. Wang, The effect of Cu addition on the electrochemical corrosion and passivation behavior of stainless steels, Electrochim. Acta 55 (2010) 5028–5035.

[50] D.K. Yadav, M. Quraishi, Electrochemical investigation of substituted pyranopyrazoles adsorption on mild steel in acid solution, Ind. Eng. Chem. Res. 51 (2012) 8194–8210.

[51] R. Padash, G.S. Sajadi, A.H. Jafari, E. Jamalizadeh, A.S. Rad, Corrosion control of aluminum in the solutions of NaCl, HCl and NaOH using 2, 6-dimethylpyridine inhibitor: experimental and DFT insights, Mater. Chem. Phys. 244 (2020), 122681.

[52] M. Mobin, I. Ahmad, M. Basik, M. Murmu, P. Banerjee, Experimental and theoretical assessment of almond gum as an economically and environmentally viable corrosion inhibitor for mild steel in 1 M HCl, Sustainable Chem. Pharm. 18 (2020), 100337.